Korean J. Chem. Eng., **20**(5), 844-849 (2003)

On the Reduction Potential of Cation-exchanged Heteropolyacids (HPAs)

In Kyu Song†, Han Soo Kim and Myung-Suk Chun*

Department of Environmental & Applied Chemical Engineering, Kangnung National University, Kangwondo 210-702, Korea
*Complex Fluids Research Team, Korea Institute of Science and Technology, Seoul 130-650, Korea
(*Received 12 June 2003 • accepted 31 July 2003*)

Abstract−UV-Visible spectroscopy and scanning tunneling microscopy (STM) studies were performed to explore reduction potentials of cation-exchanged Keggin-type heteropolyacid (HPA) catalysts. Absorption band edge and negative differential resistance (NDR) peak voltage of cation-exchanged HPA samples determined by UV-Visible spectroscopy and STM, respectively, were colsely related to their reduction potentials. It was observed that HPAs with higher reduction potentials showed absorption band edges at longer wave lengths and exhibited NDR peak voltages at less negative applied values. The reduction potentials of cation-exchanged HPA catalysts could also be correlated with the electronegativities of counter-cations. Substitution of more electronegative counter-cations increased reduction potentials of the HPAs. The NDR peak voltage and the absorption band edge of HPAs could be utilized as a correlating parameter for their reduction potentials.

Key words: Heteropolyacid (HPA), Reduction Potential, NDR, Absorption Edge

INTRODUCTION

Heteropolyacids (HPAs) are early transition metal oxygen anion clusters that exhibit a wide range of molecular sizes, compositions, and architectures [Pope and Müller, 1994]. Among various HPA structural classes, the Keggin-type [Keggin, 1933] HPAs have been widely employed as catalysts in homogeneous and heterogeneous systems for acid-base and oxidation reactions [Song et al., 1991; Kozhevnikov, 1995; Hill and Prosser-McCartha, 1995; Lee et al., 1997; Choi et al., 2000; Park et al., 2000; Lee and Song, 2000].

The catalytic redox activity of HPAs has attracted much attention [Misono, 1987; Song et al., 1991; Kim et al., 1991]. HPAs as oxidation catalysts were tested to make useful chemicals directly from hydrocarbon raw materials, including oxidation of propane to acrylic acid [Mizuno et al., 1995; Song et al., 2003; Barteau et al., 2003], and oxidation of isobutane to methacrolein and methacrylic acid [Mizuno et al., 1994, 1995]. Some theoretical and instrumental techniques have been employed to determine the reduction potential (oxidizing power) of HPAs. Quantum chemical molecular orbital studies are one of these examples that attempt to elucidate the reduction potential of HPAs [Eguchi et al., 1988; Weber, 1994]. Electrochemical reduction potential data for some series of HPAs in solutions have also been reported. These examples include heteroatom-substituted HPAs [Pope and Varga Jr., 1966; Altenau et al., 1975; Eguchi et al., 1988; Okuhara et al., 1996], polyatom-substituted HPAs [Altenau et al., 1975; Keita and Nadjo, 1989; Stobbe-Kreemers, 1993], and various HPA samples under different measurement conditions [Alimarin et al., 1980].

Another promising approach is to determine the reduction potential of HPA catalysts from negative differential resistance (NDR) peak in tunneling spectra measured with scanning tunneling microscopy (STM) [Kaba et al., 1996, 1997; Song et al., 1997, 1998; Kinne and Barteau, 2000; Song and Barteau, 2002; Song et al., 2002]. Absorption edge in the UV-Visible spectrum of HPA was also reported to reflect the reduction potential of HPA catalyst [Melsheimer et al., 1999].

Reported in this work are UV-Visible spectroscopy and scanning tunneling microscopy (STM) studies on the cation-exchanged HPAs to explore their reduction potentials. Absorption band edges determined by UV-Visible spectroscopy and negative differential resistance (NDR) peak voltage of cation-exchanged HPA samples measured by STM were correlated with the reduction potentials of the HPAs. The effect of electronegativity of counter-cation on the reduction potential, NDR peak voltage, and absorption band edge of HPAs was also investigated.

EXPERIMENTAL

1. Materials

A set of cation-exchanged $RPMo_{12}O_{40}$ ($R=H_3$, Bi_1, $Cu_{3/2}$, Cs_3) HPAs was examined with the aim of covering a wide range of electronegativity of counter-cations. Commercially available $H_3PMo_{12}O_{40}$ was purchased from Aldrich Chemical Co. Cation-exchanged HPAs were prepared by replacing all protons of $H_3PMo_{12}O_{40}$ with metal atoms, according to published methods [Ai, 1982]. Approximately 0.01 M aqueous solutions of each HPA sample were prepared. A drop of solution was deposited on a freshly cleaved graphite (HOPG) surface and allowed to dry in air for ca. 1 h at room temperature for STM imaging and tunneling spectroscopy measurements.

2. Spectroscopy Measurements

STM images were obtained in air by using a Topometrix TMX 2010 instrument. Scanning was done in the constant current mode at a positive sample bias of 100 mV and tunneling current of 1-2 nA. Both Topometrix TMX 2010 and LK Technologies LK-1000 STM instruments were used to confirm consistency and reproducibility

†To whom correspondence should be addressed.
E-mail: inksong@kangnung.ac.kr
‡This paper is dedicated to Professor Hyun-Ku Rhee on the occasion of his retirement from Seoul National University.

of tunneling spectra. To measure a tunneling spectrum, the sample bias was ramped from −2 to +2 V with respect to the tip and the tunneling current was monitored. The voltage axis in the tunneling spectrum represents the potential applied to the sample relative to that of the tip. Tunneling spectroscopy measurements were performed at least ten times each with at least three different tips for each sample to obtain more reproducible results and to provide a basis for statistical analyses.

HPA samples were calcined at 300 °C with an air stream to eliminate water molecules, prior to UV-Visible spectrocopy measurements. UV-Visible spectroscopy measurements of cation-exchanged HPAs in solids were performed with a Ramada 20 Spectrometer (Perkin-Elmer) within the range from 200 to 900 nm at a scan rate of 120 nm/min.

RESULTS AND DISCUSSION

1. NDR Peak Voltage of Cation-exchanged HPAs

Fig. 1(a) shows the molecular structure of the pseudo-spherical (T_d symmetry) Keggin-type $[PMo_{12}O_{40}]^{3-}$ heteropolyanion constructed from X-ray crystallography data [Strandberg, 1975; Brown et al., 1977]. The molecular structure of $[PMo_{12}O_{40}]^{3-}$ consists of a heteroatom, P, at the center of the anion cluster, tetrahedrally coordinated to four oxygen atoms. This tetrahedron is surrounded by twelve MoO_6 octahedra. The van der Waals diameter along the 3-fold axis of symmetry is ca. 11 Å. Fig. 1(b) shows the three-dimensional array of HPAs comprising heteropolyanions, protons, cations, water, and/or organic molecules, called the secondary structure [Misono, 1987]. The counter-cations are located in the interstitial spaces between heteropolyanions. It is known that the redox properties of HPAs can be tuned by changing the identity of counter-cations, heteroatoms, and framework metal atoms (polyatoms) [Song et al., 1991, 1997; Okuhara et al., 1996].

Fig. 1(c) shows the STM image of an $H_3PMo_{12}O_{40}$ array on graphite. The STM image clearly shows the formation of a self-assembled and well-ordered array on the graphite surface. The periodicity constructed on the basis of lattice constants determined from two-dimensional fast Fourier Transform (2-D FFT) is 10.8 Å. The measured periodicity is in good agreement with lattice constants of the Keggin-type HPAs obtained by STM [Kaba et al., 1996, 1997; Song et al., 1997, 1998, 2002; Kinne and Barteau, 2000; Song and Barteau, 2002] and X-ray crystallography [Strandberg, 1975; Brown et al., 1977].

Fig. 1(d) shows the typical tunneling spectra taken at two differ-

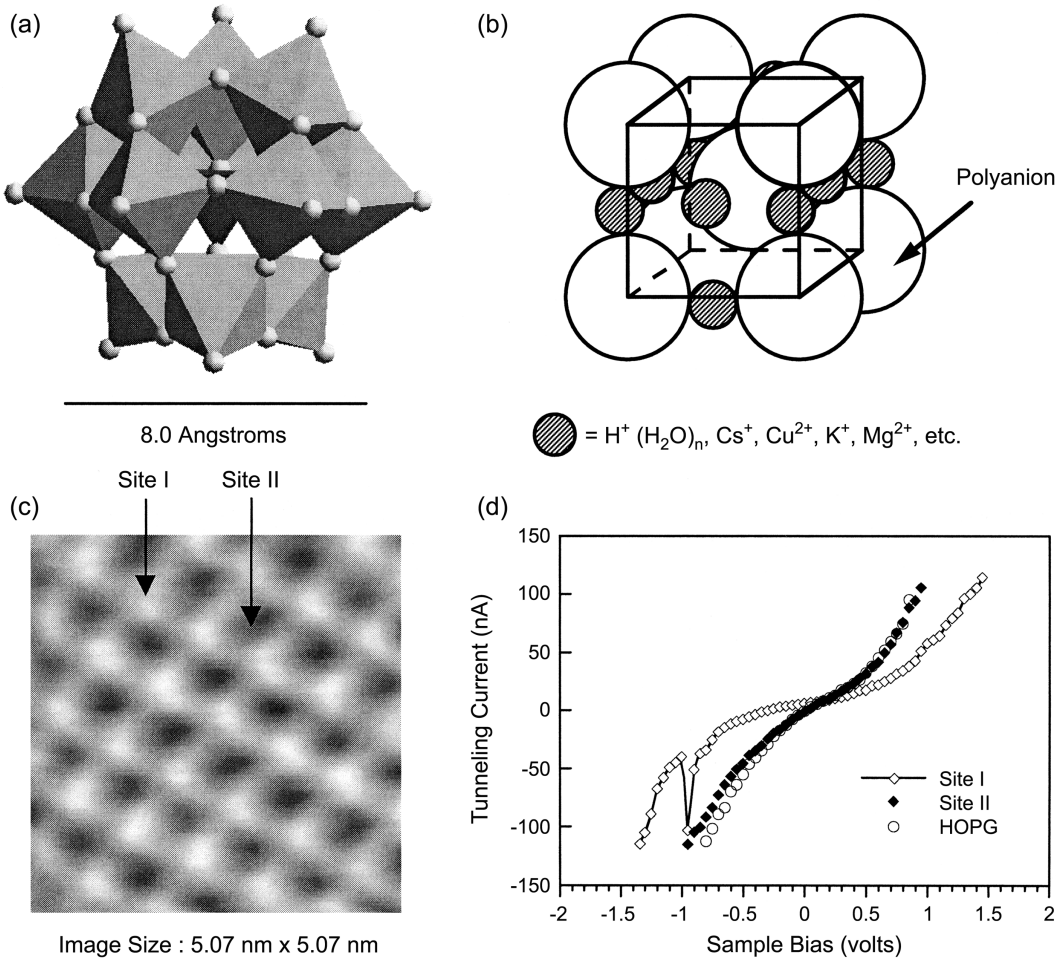

Fig. 1. (a) Polyhedral representation of the molecular structure of the pseudo-spherical Keggin-type $[PMo_{12}O_{40}]^{3-}$ heteropolyanion (primary structure), (b) schematic of the secondary structure of HPAs, (c) STM image of $H_3PMo_{12}O_{40}$ deposited on graphite, and (d) current-voltage spectra taken at two different sites in Fig. 1(c).

ent sites, denoted as Site I and Site II in the image of $H_3PMo_{12}O_{40}$ array in Fig. 1(c). The spectrum taken at a position corresponding to the bright corrugation (Site I) exhibits distinctive current-voltage (I-V) behavior, referred to as negative differential resistance (NDR). The NDR behavior is manifested as local maxima and minima in the I-V spectrum. Such peaks in the I-V spectrum result in negative values of dI/dV, and thus the phenomenon is referred to as NDR. The NDR peak voltage was defined as the voltage at which the maximum current was observed in this region. The NDR peak voltage of bright corrugation (HPA molecule) in Fig. 1(c) was found to be −0.95 V. A tunneling spectrum taken at the interstitial space (Site II) between bright corrugations showed the same I-V response as bare graphite, indicating that the two-dimensional array of $H_3PMo_{12}O_{40}$ on graphite is a monolayer, as previously demonstrated [Kaba et al., 1996, 1997; Song et al., 1997, 1998, 2002; Kinne and Barteau, 2000; Song and Barteau, 2002]. The NDR measurements atop the bright corrugations (Site I) were carried out several times with at least three different tips to obtain more accurate and reproducible results, and to provide a basis for statistical analyses. It was observed that NDR peak voltages of the $H_3PMo_{12}O_{40}$ sample showed a monomodal distribution with a statistical average of −0.95±0.09 V. The most reproducible and representative NDR peak voltage of each HPA sample examined in this work was determined by this statistical method, as described previously [Song and Barteau, 2002].

The NDR peak voltages of cation-exchanged HPA samples are listed in Table 1, together with Tanaka electronegativities of counter-cations [Tanaka and Ozami, 1967]. The Tanaka electronegativity takes into account the electron-donating and -accepting ability of the atom. As listed in Table 1, it is clear that the NDR peak voltage of cation-exchanged HPA sample appeared at less negative value with increasing electronegativity of counter-cation.

2. UV-Visible Absorption Band Edge

Fig. 2 shows the UV-Visible spectra of cation-exchanged HPA samples. Fig. 2 also shows the absorption band edge for $H_3PMo_{12}O_{40}$ sample. The absorption band edge was defined by extrapolating the region of steep descent in the spectrum to zero absorbance. The absorption band edge of $H_3PMo_{12}O_{40}$ catalyst was determined to be 516 nm, as shown in Fig. 2(a). The absorption band edges of cation-exchanged HPA samples are summarized in Table 2, together with Tanaka electronegativities of counter-cations [Tanaka and Ozami, 1967]. Clearly, Table 2 shows that the absorption band edge of HPA sample appeared at longer wave length with increasing Tanaka electronegativity of counter-cation.

3. Correlation between NDR Peak Voltage and Reduction Potential

Table 1. NDR peak voltages of cation-exchanged HPA samples and Tanaka electronegativities of counter-cations

HPA catalyst	Tanaka electronegativity of counter-cation[1)]	NDR peak voltage (volts)
$Cs_3PMo_{12}O_{40}$	2.27	−1.50
$H_3PMo_{12}O_{40}$	6.60	−0.95
$Cu_{3/2}PMo_{12}O_{40}$	9.50	−0.72
$Bi_1PMo_{12}O_{40}$	14.14	−0.60

[1)]Defined as $(1+2Z)X_o$, where Z and X_o represent charge and Pauling scale electronegativity of the metal ion, respectively.

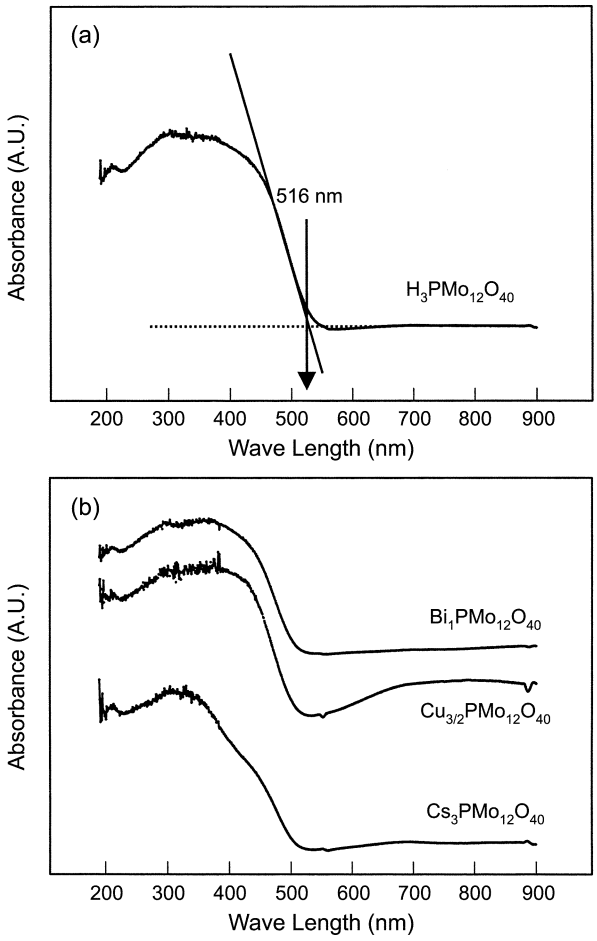

Fig. 2. UV-Visible spectra of cation-exchanged HPA samples.

Table 2. Absorption band edges of cation-exchanged HPA samples and Tanaka electronegativities of counter-cations

HPA catalyst	Tanaka electronegativity of counter-cation	Absorption band edge (nm)
$Cs_3PMo_{12}O_{40}$	2.27	496
$H_3PMo_{12}O_{40}$	6.60	516
$Cu_{3/2}PMo_{12}O_{40}$	9.50	519
$Bi_1PMo_{12}O_{40}$	14.14	524

A previous work [Ai, 1982] has shown that the reduction potential of $H_3PMo_{12}O_{40}$ measured in solids increased when the protons of the $H_3PMo_{12}O_{40}$ were replaced by more electronegative cations such as Cu^{2+}; the reduction potential decreased when the protons were replaced by less electronegative cations such as Cs^+. This means that electronegativity of counter-cation plays a very important role in determining the reduction potential of HPAs. In other words, reduction potentential of the cation-exchanged HPAs can be controlled by the electronegativity of the counter-cation.

Fig. 3 shows the NDR peak voltage of HPA samples and Tanaka electronegativity of counter-cations, both plotted with respect to reduction potential of cation-exchanged HPAs. The reduction potential data measured in solids were taken from a literature [Ai, 1982]. The reduction potential of cation-exchanged HPA roughly increased,

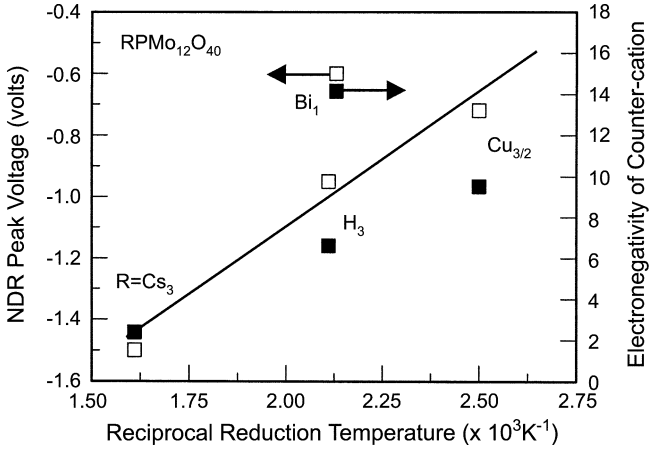

Fig. 3. NDR peak voltage of HPA samples and Tanaka electronegativity of counter-cations, both plotted with respect to reduction potential of cation-exchanged HPAs.

as the electronegativity of counter-cation increased, and as the NDR peak voltage of HPA sample appeared at less negative value. As mentioned earlier, the Tanaka electronegativity takes into account the electron-donating and -accepting ability of the atom. One possible explanation for the results in Fig. 3 is that a more electronegative cation acts as a large electron reservoir to facilitate electron transfer to the heteropolyanion in reducing environments, by providing a route for electron delocalization [Kim et al., 1991].

4. Correlation between Absorption Band Edge and Reduction Potential

The absorption band edge in the UV-Visible spectrum of an HPA sample reflects the energy needed for Ligand-to-Metal Charge Transfer (LMCT) to occur [Melsheimer et al., 1999]. This involves an electron transfer from the HOMO (Highest Occupied Molecular Orbital) to the LUMO (Lowest Unoccupied Molecular Orbital). The HOMO is almost unaffected by the changes in the Keggin framework; however, the LUMO is greatly affected by the changes in the Keggin framework [Weber, 1994]. Therefore, the absorption band edge reflects the change in the LUMO energy. The edge energy can be calculated from the absorption band edge (λ) by the equation of $E=hc/\lambda$, where h and c represent the Plank's constant and the speed of light, respectively. Therefore, the longer absorption band edge of HPA sample in Table 2 corresponds to the lower edge energy.

Fig. 4 shows the absorption band edge of HPA samples and Tanaka electronegativity of counter-cations, both plotted with respect to reduction potential of cation-exchanged HPAs. The reduction potential data measured in solids were also taken from literature [Ai, 1982]. The reduction potential of cation-exchanged HPA increased as the electronegativity of counter-cation increased, and as the absorption band edge of HPA sample appeared at longer wave length. This strongly implies that the absorption band edge of HPA sample can serve as a correlation parameter for the reduction potential of HPA.

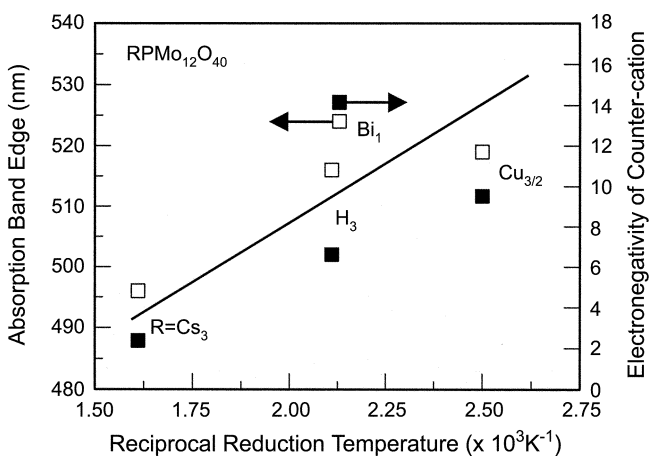

Fig. 4. Absorption band edge of HPA samples and Tanaka electronegativity of counter-cations, both plotted with respect to reduction potential of cation-exchanged HPAs.

5. Reduction Potential Dependence on NDR Peak Voltage and Absorption Band Edge

Fig. 5 shows the NDR peak voltage and absorption band edge of cation-exchanged HPAs, both plotted with respect to reduction potential of HPA samples. NDR peak voltage and absorption band

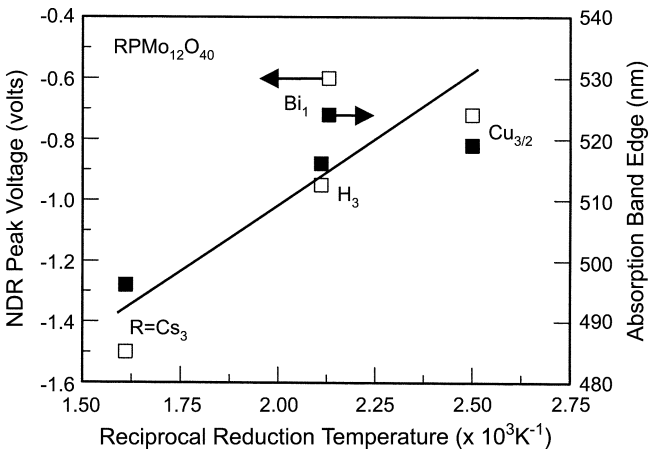

Fig. 5. NDR peak voltage and absorption band edge of cation-exchanged HPAs, both plotted with respect to reduction potential of HPA samples.

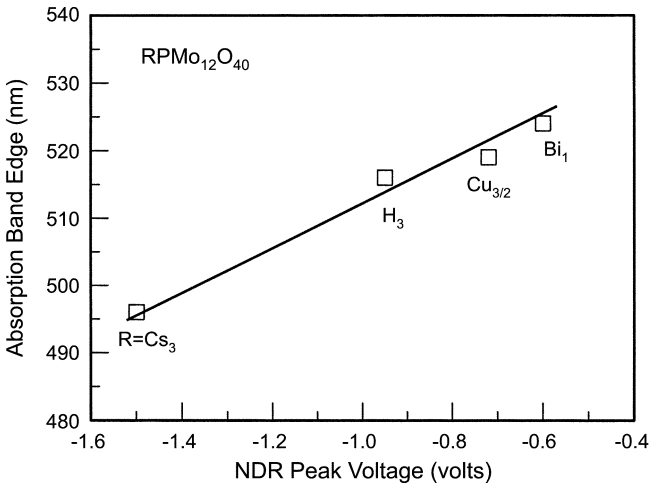

Fig. 6. Correlation between NDR peak voltage and absorption band edge of cation-exchanged HPA samples.

edge of cation-exchanged HPAs are closely related to the reduction potential of the HPA samples. Fig. 5 shows that the reduction potential of cation-exchanged HPA increased, as the NDR peak voltage appeared at less negative value, and as the absorption band edge appeared at longer wave length. Fig. 6 shows the correlation between NDR peak voltage and absorption band edge of cation-exchanged HPA samples, established from Table 1 and Table 2. This result clearly shows that NDR peak voltages of cation-exchanged HPA samples could be directly correlated with absorption band edges of these HPAs. Thus, the NDR peak voltage and the absorption band edge of cation-exchanged HPA can be used as a correlating parameter for the reduction potential of HPA catalyst.

CONCLUSIONS

In this work, UV-Visible spectroscopy and scanning tunneling microscopy (STM) studies were performed to explore reduction potentials of cation-exchanged Keggin-type HPA catalysts. It was observed that the absorption band edge determined by UV-Visible spectroscopy and the negative differential resistance (NDR) peak voltage of HPA sample measured by STM were closely related to the reduction potential of HPA and to counter-cation electronegativity. It was found that HPAs with higher reduction potential showed absorption band edges at longer lengths and exhibited NDR peaks at less negative applied voltages. As the electronegativity of counter-cation increased, NDR peak appeared at less negative voltage and absorption band edge shifted to longer wave length. Correspondingly, the reduction potential of HPA sample increased. It is concluded that the NDR peak voltage and the absorption band edge of cation-exchanged HPA can serve as a correlating parameter for the reduction potential of HPA catalyst.

ACKNOWLEDGMENTS

The authors wish to acknowledge the financial support from KOSEF (Korea Science and Engineering Foundation) for this work (R01-2001-000-00411-0).

REFERENCES

Ai, M., "Effects of Cations Introduced into 12-Molybdophosphoric Acid on the Catalyst Properties," *Appl. Catal*., **4**, 245 (1982).

Alimarin, I. P., Dorokhova, E. N., Kazanskii, L. P. and Prokhorova, G. V., "Electrochemical Methods in the Analytical Chemistry of Heteropoly Compounds," *Zh. Anal. Khim*., **35**, 2000 (1980).

Altenau, J. J., Pope, M. T., Prados, R. A. and So, H., "Models for Heteropoly Blues. Degree of Valence Trapping in Vanadium(IV)- and Molybdenum(V)-substituted Keggin Anions," *Inorg. Chem*., **14**, 417 (1975).

Barteau, M. A., Lyons, J. E. and Song, I. K., "Surface Chemistry and Catalysis on Well-defined Oxide Surfaces: Nanoscale Design Bases for Single-site Heterogeneous Catalysts," *J. Catal*., **216**, 236 (2003).

Brown, G. M., Noe-Spirlet, M. R., Busing, W. R. and Levy, H. A., "Dodecatungstophosphoric Acid Hexahydrate, $(H_5O_2^+)_3(PW_{12}O_{40}^{3-})$. The True Structure of Keggin's Pentahydrate from Single-crystal X-ray and Neutron Diffraction Data," *Acta. Cryst. B*, **33**, 1038 (1977).

Choi, J. S., Song, I. K. and Lee, W. Y., "A Composite Catalytic Membrane Reactor Using Heteropolyacid-blended Polymer Membrane," *Korean J. Chem. Eng*., **17**, 280 (2000).

Eguchi, K., Seiyama, T., Yamazoe, N., Katsuki, S. and Taketa, H., "Electronic Structures of $XMo_{12}O_{40}$ Heteropolyanions (X=P, As, Si, and Ge) and Their Reduction Behavior," *J. Catal*., **111**, 336 (1988).

Hill, C. L. and Prosser-McCartha, C. M., "Homogeneous Catalysis by Transition Metal Oxygen Anion Clusters," *Coord. Chem. Rev.*, **143**, 407 (1995).

Kaba, M. S., Song, I. K. and Barteau, M. A., "Investigation of Framework and Cation Substitutions in Keggin-type Heteropoly Acids Probed by Scanning Tunneling Microscopy and Tunneling Spectroscopy," *J. Vac. Sci. Technol. A*, **15**, 1299 (1997).

Kaba, M. S., Song, I. K. and Barteau, M. A., "Ordered Array Formation and Negative Differential Resistance Behavior of Cation-exchanged Heteropoly Acids Probed by Scanning Tunneling Microscopy," *J. Phys. Chem*., **100**, 19577 (1996).

Keggin, J. F., "Structure of the Molecule of 12-Phosphotungstic Acid," *Nature*, **131**, 908 (1933).

Keita, B. and Nadjo, L., "New Oxometalate-based Materials for Catalysis and Electrocatalysis," *Mater. Chem. Phys*., **22**, 77 (1989).

Kim, H. C., Moon, S. H. and Lee, W. Y., "Nature of the Effect of Counter Cations on the Redox Property of 12-Molybdophosphates," *Chem. Lett*., 447 (1991).

Kinne, M. and Barteau, M. A., "STM and TS Investigations of Silver Polyoxometalate Monolayers: Model Compounds and Potential Multifunctional Oxidation Catalysts," *Surf. Sci*., **447**, 105 (2000).

Kozhevnikov, I. V., "Heteropoly Acids and Related Compounds as Catalysts for Fine Chemical Synthesis," *Catal. Rev.-Sci. Eng*., **37**, 311 (1995).

Lee, W. Y. and Song, I. K., "Design of Heteropolyacid-imbedded Polymer Films and Catalytic Membranes," *HWAHAK KONGHAK*, **38**, 317 (2000).

Lee, W. Y., Song, I. K., Lee, J. K., Park, G. I. and Lim, S. S., "Design of Heteropoly Compound-imbedded Polymer Film Catalysts and Their Application," *Korean J. Chem. Eng*., **14**, 432 (1997).

Melsheimer, J., Mahmoud, S. S., Mestl, G. and Schlögl, R., "In Situ UV-Vis Diffuse Reflectance Spectroscopy of Reduction-reoxidation of Heteropoly Compounds by Methanol and Ethanol: A Correlation between Spectroscopic and Catalytic Data," *Catal. Lett*., **60**, 103 (1999).

Misono, M., "Heterogeneous Catalysis by Heteropoly Compounds of Molybdenum and Tungsten," *Catal. Rev.-Sci. Eng*., **29**, 269 (1987).

Mizuno, N., Iwamoto, M. and Tateishi, M., "Pronounced Catalytic Activity of $Fe_{0.08}Cs_{2.5}H_{1.26}VMo_{11}O_{40}$ for Direct Oxidation of Propane into Acrylic Acid," *Appl. Catal. A*, **128**, 1165 (1995).

Mizuno, N., Suh, D.-J., Han, W. and Kudo, T., "Catalytic Performance of $Cs_{2.5}Fe_{0.08}H_{1.26}VMo_{11}O_{40}$ for Direct Oxidation of Lower Alkanes," *J. Mol. Catal. A*, **128**, 309 (1995).

Mizuno, N., Tateishi, M. and Iwamoto, M., "Direct Oxidation of Isobutane into Methacrylic Acid and Methacrolein over $Cs_{2.5}Ni_{0.08}$-substituted $H_3PMo_{12}O_{40}$," *J. Chem. Soc. Chem. Comm*., 1411 (1994).

Okuhara, T., Mizuno, N. and Misono, M., "Catalytic Chemistry of Heteropoly Compounds," *Adv. Catal*., **41**, 113 (1996).

Park, G. I., Lee, W. Y. and Song, I. K., "MTBE Synthesis by Keggin-type and Dawson-type Heteropolyacids," *HWAHAK KONGHAK*, **38**, 155 (2000).

Pope, M. T. and Müller, A. (Eds.), "Polyoxometalates: From Platonic

Solids to Anti-retroviral Activity," Kluwer Academic Publishers, Dordrecht, The Netherlands (1994).

Pope, M. T. and Varga Jr., G. M., "Heteropoly Blues: I. Reduction Stoichiometries and Reduction Potentials of Some 12-Tungstates," *Inorg. Chem*., **5**, 1249 (1966).

Song, I. K., Kaba, M. S., Barteau, M. A. and Lee, W. Y., "Investigation of Redox Potential and Negative Differential Resistance Behavior of Heteropolyacids by Scanning Tunneling Microscopy," *Catal. Today*, **44**, 285 (1998).

Song, I. K., Kaba, M. S., Barteau, M. A. and Lee, W. Y., "Scanning Tunneling Microscopy of Self-assembled Heteropoly Acid Monolayers Deposited on Graphite Surface: NDR Behavior and Redox Activity," *HWAHAK KONGHAK*, **35**, 407 (1997).

Song, I. K. and Barteau, M. A., "Scanning Tunneling Microscopy and Tunneling Spectroscopy of Heteropolyacid Self-assembled Monolayers: Connecting Nano Properties to Bulk Properties," *Korean J. Chem. Eng*., **19**, 567 (2002).

Song, I. K., Lyons, J. E. and Barteau, M. A., "Correlation of Alkane Oxidation Performance with STM and Tunneling Spectroscopy Measurements of Heteropolyacid Catalysts," *Catal. Today* (2003): in press.

Song, I. K., Moon, S. H. and Lee, W. Y., "Catalytic Properties of Thermally Decomposed 12-Molybdophosphoric and 10-Molybdo-2-vanadophosphoric Acids," *Korean J. Chem. Eng*., **8**, 33 (1991).

Song, I. K., Shnitser, R. B., Cowan, J. J., Hill, C. L. and Barteau, M. A., "Nanoscale Characterization of Redox and Acid Properties of Keggin-type Heteropolyacids by Scanning Tunneling Microscopy and Tunneling Spectroscopy: Effect of Heteroatom Substitution," *Inorg. Chem*., **41**, 1292 (2002).

Stobbe-Kreemers, A. W., "The Development of Heterogeneous Wacker Oxidation Catalysis: The Role of the Support and the Redox Component," Ph.D Thesis, Delft Univ. (1993).

Strandberg, R., "Multicomponent Polyanions. 13. The Crystal Structure of a Hydrated Dodecamolybdophosphoric Acid, $H_3Mo_{12}PO_{40}(H_2O)_{29\text{-}31}$," *Acta Chem. Scand. A*, **29**, 359 (1975).

Tanaka, K. and Ozami, A., "Acid-Base Properties and Catalytic Activity of Solid Surfaces," *J. Catal*., **8**, 1 (1967).

Weber, R. S., "Molecular Orbital Study of C-H Bond Breaking during the Oxidative Dehydrogenation of Methanol Catalyzed by Metal Oxide Surfaces," *J. Phys. Chem*., **98**, 2999 (1994).